

NON-GAUSSIAN SIGNATURE INDUCED BY THE SZ EFFECT OF GALAXY CLUSTERS

N. AGHANIM & O. FORNI

*Institut d'Astrophysique Spatiale, Bât. 121, Université Paris Sud,
91405 Orsay Cedex, France*



We apply statistical tests, based on the study of the coefficients in a wavelet decomposition, to a cosmological signal: the Cosmic Microwave Background (CMB) anisotropies. The latter represent the superposition of primary anisotropy imprints of the initial density perturbations and secondary anisotropies due to photon interactions after recombination. In an inflationary scenario with Gaussian distributed fluctuations, we study the statistical signature of the secondary effects. More specifically, we investigate the dominant effects arising from the Sunyaev-Zel'dovich effect of galaxy clusters. Our study predicts the non-Gaussian signature of these secondary anisotropies and its detectability in the context of the future CMB satellite Planck Surveyor.

1 Introduction

One of the major goals of cosmology is to understand the origin of the initial density perturbations. Do they come from inflation⁴ or from topological defects⁸? One way to answer this question is to make a statistical analysis of the CMB anisotropies. In fact, inflation predicts a Gaussian distribution of the primary anisotropies whereas the topological defects predict a non-Gaussian distribution. However, not only topological defects produce non-Gaussian signals. There are other astrophysical sources of non-gaussianity such as gravitational lensing (cf. F. Bernardeau's contribution in this proceedings) and the secondary anisotropies such as the Sunyaev-Zel'dovich effect⁷ of galaxy clusters.

In this context, we have developed a method for the statistical analysis based on the wavelet decomposition of a signal. The method has been tested on an arbitrary set of Gaussian and non-Gaussian maps and then applied to CMB simulated maps to investigate the effect of the SZ contribution on the statistical signature of the anisotropies.

2 Detection method

Our method is based on a wavelet analysis of an image. That is, rather than analysing the signal in the direct space, we analyse the associated coefficients in the wavelet decomposition. The wavelet analysis can be viewed as a convolution of the signal by band pass filters: a scaling function similar to a low pass filter and a wavelet function similar to a high pass filter. The low pass filter will give an image with a lower resolution and the high pass will give the associated details. We have used the multi-scale wavelet analysis⁵ to decompose an input signal into a series of successive low resolution images and their associated detail images. At each level of the decomposition, the reference image has a resolution reduced by a factor of two and only this reference low pass image is decomposed at each level. This is the principle of the dyadic decomposition. We have chosen an anti-symmetric wavelet⁹ function similar to a first derivative operator because we expect that the non-Gaussian signatures arise from sharp gradients in the signal. Such a function is particularly sensitive to gradients and will detect them easily. The high pass filter applied to both directions of the image gives at each level three detail images corresponding to vertical, horizontal and diagonal details. The features of interest, particularly the statistical signatures, are studied at each scale (or level) for each type of details. We have qualified and tested our detection method on a set of Gaussian and non-Gaussian maps (100 of each) having the same power spectrum. This condition allows us to attribute the differences that are detected between the Gaussian and non-Gaussian maps to nothing but their statistical nature.

Our detection method³ is based on the three following major steps. First, we perform the wavelet decomposition of both 100 Gaussian maps and 100 non-Gaussian maps. We thus obtain at each decomposition level the wavelet coefficients associated with the vertical, horizontal and diagonal details. We also define the multi-scale gradient as the sum of the squared coefficients associated with the vertical and horizontal details. The non-Gaussian signature can be detected through the third or fourth order moment of the distribution, respectively the skewness and the kurtosis. In the following, we focus only on the excess of kurtosis because our signals are very moderately skewed. The second step of the method is to compute for each Gaussian and non-Gaussian map and at each level the excess of kurtosis of the wavelet coefficients associated with the corresponding details. We check that contrary to the Gaussian maps, the excess of kurtosis of the non-Gaussian signal is always centred around a non-zero value. We also note that the dispersion around the mean excess of kurtosis increases at high decomposition levels even for the Gaussian maps, due to the lack of coefficients at these levels. Therefore, in the following, we restrict our study to the first three levels.

The last step of the analysis is to quantify the detectability of the non-Gaussian signature. This is done by comparing the probability distribution functions (PDF) of the different processes. We compute the median excess of kurtosis of the 100 non-Gaussian maps at each decomposition scale and estimate the probability that it belongs to the PDF of the Gaussian maps. A low probability favours of a non-Gaussian signal whereas a high probability indicates a Gaussian process. We can also perform a more global comparison of the PDFs through the Kolmogorov-Smirnov test⁶. It gives, with a very good accuracy, the probability for a distribution to be different from a Gaussian.

3 Application to CMB

We apply our method to simulated CMB data including primary and secondary anisotropies. Our goal is to estimate the statistical non-Gaussian contamination induced by the secondary anisotropies. Therefore, we use an inflation model that generates Gaussian distributed primary anisotropies to which we add the simulated² contributions due to the Sunyaev-Zel'dovich

Scale		k_1	σ_+	σ_-		k_2	σ_+	σ_-
I	$\partial/\partial x$	13.89	11.67	3.97		11.98	7.66	3.74
II	$\&$	2.90	1.29	0.48	$\partial^2/\partial x\partial y$	6.88	7.00	1.73
III	$\partial/\partial y$	0.09	0.08	0.08		0.36	0.17	0.11

Table 1: The median excess of kurtosis, at four decomposition scales, computed over 100 realisations of the sum of CMB and secondary anisotropies (inhomogeneous re-ionisation¹ and thermal and kinetic SZ effect). The signal includes the Gaussian noise expected for the Planck mission. k_1 is the median excess computed with the coefficients associated with the vertical and horizontal gradients, and k_2 is given for the diagonal details. The σ values are the boundaries of the confidence interval for one statistical realisation.

(thermal and kinetic) effect of galaxy clusters.

We have simulated 100 statistical realisations of the resulting CMB maps and performed the multi-scale decomposition. Following our proposed method, we compute the excess of kurtosis at different scales for the coefficients associated with the diagonal, vertical and horizontal details (Table 1).

At the first three decomposition scales, the excess of kurtosis is very large due to the SZ contribution. We also note, that the computations using the diagonal details are more sensitive to non-gaussianity and thus more powerful in detecting it. In fact, the galaxy clusters exhibit very peaked profiles or even point-like behaviour. The diagonal details are very sensitive to symmetric profiles. We find that the SZ effect a major source of non-gaussianity among the secondary effects.

4 Effects of the instrumental configurations

We apply our statistical discriminators to test for non-gaussianity within the context of the representative instrumental configuration of the future Planck Surveyor satellite for CMB observations.

We use the same astrophysical contributions as those described above (primary and SZ). The difference lies in the fact that the maps are convolved with a 6 arcminute Gaussian beam. We also take into account the expected Gaussian noise of Planck $((\delta T/T)_{rms} \sim 2 \cdot 10^{-6}$ per 1.5 arcminute pixel). The convolution by a 6 arcminute beam suppresses the power at the corresponding scale (Scale I) and affects the second decomposition scale whereas the third is not significantly altered. At the third decomposition scale, we find for the multi-scale gradient $k = 0.62^{+1.43}_{-0.60}$. Whereas we find for the horizontal and vertical details, and for the diagonal details respectively, $k = 0.07^{+0.11}_{-0.08}$ and 0.16 ± 0.10 . In order to quantify the detectability of non-gaussianity in the Planck-like configuration, we generate Gaussian distributed maps with same power spectrum as the studied signal. We plot (Fig. 1) the PDF of the Gaussian (dashed line) and non-Gaussian (solid line) processes. We derive the probability that the median excess of kurtosis measured on the “real sky” belongs to the Gaussian process. Using the multi-scale gradient, we find that the probability of detecting non-gaussianity is 71.9% at the second decomposition scale. There is no significant detection elsewhere. Whereas using the coefficients of the diagonal details, the probability of detecting a non-Gaussian signature at the third scale is 94.5%. We apply the K-S test to the distribution of the excess of kurtosis for the diagonal details and find a probability of 96.6% of detecting non-gaussianity. Since the comparison of the two distributions using the K-S test is very sensitive to departures from gaussianity. It thus gives better results on the detection of the non-Gaussian signature.

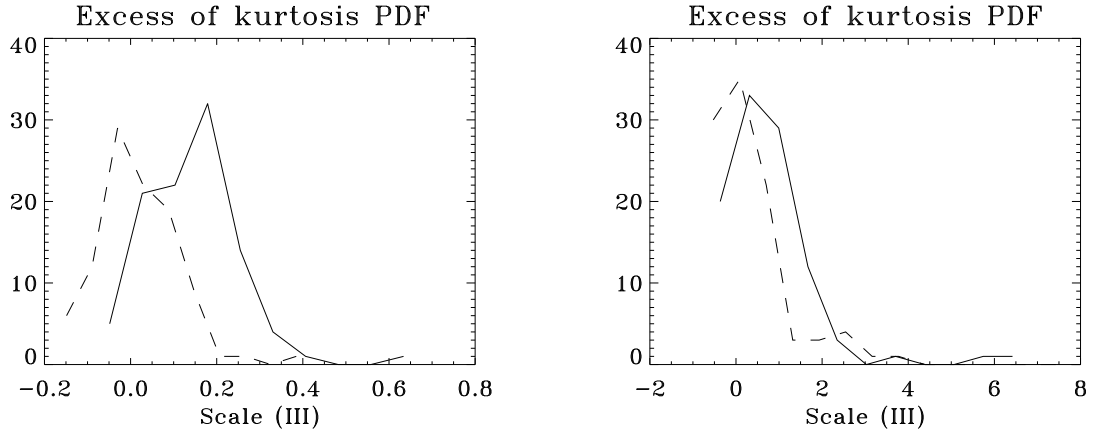


Figure 1: For the Planck-like configuration (CMB + SZ + inhomogeneous re-ionisation), probability distribution functions, as percentages, of the excess of kurtosis computed with the multi-scale gradient coefficients (right panels) and with the coefficients of the diagonal details (left panels). The dashed line is for the Gaussian test maps with same power spectrum as the non-Gaussian signal (solid line).

5 Conclusions

In the present study, we investigate the statistical signature induced by the SZ effect of galaxy clusters when the primary anisotropies result from an inflationary scenario and are thus Gaussian distributed. We use discriminators based on the statistical properties of the coefficients in a four level wavelet decomposition. In our study, we find that the SZ effect of clusters generates a very large non-Gaussian signature that dominates by far all other secondary anisotropies. We apply our statistical tests to a Planck-like configuration in order to estimate the capabilities of the satellite to detect the non-Gaussian signature of the SZ effect. In this case, we detect unambiguously the non-Gaussian signature at the third decomposition scale ($\simeq 12$ arcminutes), the first ($\simeq 3$ arcminutes) and second ($\simeq 6$ arcminutes) scales being affected by the beam convolution.

References

1. N. Aghanim *et al.*, *A&A* **311**, 1 (1996).
2. N. Aghanim *et al.*, *A&A* **334**, 409 (1998).
3. O. Forni and N. Aghanim, *A&ASuppl. Ser.* **137**, 553 (1999)
4. A. Guth, *Phys. Rev. D* **23**, 347 (1981)
5. S. Mallat, *IEEE Trans. Patt. Anal. Machine Intell.* **7**, 674 (1989)
6. W. H. Press *et al.*, in *Numerical Recipes* (1992)
7. R. A Sunyaev and I. B. Zel'dovich, *ARA&A* **18**, 537 (1980)
8. A. Vilenkin, *Phys. Rep.* **121**,263 (1985)
9. Villasenor *et al.*, *IEEE Trans. Image Proc.* **4**, 1053 (1995)